Computer-aided analysis of star shot films for high-accuracy radiation therapy treatment units

2012 Phys. Med. Biol. 57 2997

(http://iopscience.iop.org/0031-9155/57/10/2997)

IOP Publishing Physics in Medicine and Biology

Phys. Med. Biol. **57** (2012) 2997–3011 doi:10.1088/0031-9155/57/10/2997

Computer-aided analysis of star shot films for high-accuracy radiation therapy treatment units

Tom Depuydt[1,7], Rudi Penne[2], Dirk Verellen[1], Jan Hrbacek[3], Stephanie Lang[3], Katrien Leysen[1], Iwein Vandevondel[1], Kenneth Poels[1], Truus Reynders[1], Thierry Gevaert[1], Michael Duchateau[1], Koen Tournel[1], Marlies Boussaer[1], Dorian Cosentino[4], Cristina Garibaldi[5], Timothy Solberg[6] and Mark De Ridder[1]

[1] Radiotherapy Department, UZ Brussel, Vrije Universiteit Brussel, Brussels, Belgium
[2] Departement Wiskunde, Universiteit Antwerpen en Departement IWT, Karel de Grote-Hogeschool, Antwerpen, Belgium
[3] UniversitätsSpital Zürich, Zürich, Switzerland
[4] Ospedale Sant'Anna, Via Ravona, 22020 San Fermo della Battaglia, Como, Italy
[5] Radiation Oncology Department, European Institute of Oncology, Milan, Italy
[6] University of Texas Southwestern Medical Center, Dallas, Texas, USA

E-mail: tom.depuydt@uzbrussel.be

Received 4 November 2011, in final form 4 March 2012
Published 26 April 2012
Online at stacks.iop.org/PMB/57/2997

Abstract

As mechanical stability of radiation therapy treatment devices has gone beyond sub-millimeter levels, there is a rising demand for simple yet highly accurate measurement techniques to support the routine quality control of these devices. A combination of using high-resolution radiosensitive film and computer-aided analysis could provide an answer. One generally known technique is the acquisition of star shot films to determine the mechanical stability of rotations of gantries and the therapeutic beam. With computer-aided analysis, mechanical performance can be quantified as a radiation isocenter radius size. In this work, computer-aided analysis of star shot film is further refined by applying an analytical solution for the smallest intersecting circle problem, in contrast to the gradient optimization approaches used until today. An algorithm is presented and subjected to a performance test using two different types of radiosensitive film, the Kodak EDR2 radiographic film and the ISP EBT2 radiochromic film. Artificial star shots with *a priori* known radiation isocenter size are used to determine the systematic errors introduced by the digitization of the film and the computer analysis. The estimated uncertainty on the isocenter size measurement with the presented technique was 0.04 mm (2σ) and 0.06 mm (2σ) for radiographic and radiochromic films, respectively. As an application of the technique, a study was conducted to compare the mechanical stability of O-ring gantry systems with C-arm-based gantries. In

[7] Author to whom any correspondence should be addressed.

total ten systems of five different institutions were included in this study and star shots were acquired for gantry, collimator, ring, couch rotations and gantry wobble. It was not possible to draw general conclusions about differences in mechanical performance between O-ring and C-arm gantry systems, mainly due to differences in the beam–MLC alignment procedure accuracy. Nevertheless, the best performing O-ring system in this study, a BrainLab/MHI Vero system, and the best performing C-arm system, a Varian Truebeam system, showed comparable mechanical performance: gantry isocenter radius of 0.12 and 0.09 mm, respectively, ring/couch rotation of below 0.10 mm for both systems and a wobble of 0.06 and 0.18 mm, respectively. The methodology described in this work can be used to monitor mechanical performance constancy of high-accuracy treatment devices, with means available in a clinical radiation therapy environment.

1. Introduction

Modern radiation treatment units show highly accurate mechanical performance. Current state-of-the-art radiation treatment delivery techniques use large numbers and various combinations of gantry, treatment couch and collimator angles to optimize target coverage and minimize the exposure of surrounding healthy tissues. The device is assumed by the treatment planning systems to have infinite mechanical rigidity and to be perfectly mechanically calibrated. The treatment planning process does account for mechanical imperfections with a contribution to setup uncertainties in the CTV-to-PTV margin (ICRU Report 83 2010). Accurate measurement of these mechanical distortions can lead to better calculation of these margins. For the last generation of radiation therapy treatment devices, mechanical distortions are indeed less significant compared to the other, mainly patient-related, uncertainties (van Herk *et al* 2004). However, with advances in treatment planning and delivery techniques aiming at improved accuracy of the treatment, the machine accuracy will become of considerable importance, certainly in advanced high-precision radiation therapy and radiosurgery.

A radiation therapy treatment unit consists of a mechanical gantry on which a linear accelerator is mounted. To shape the therapeutic beam, a set of collimation devices is attached to the gantry. Depending on the design of the treatment unit, both the gantry, the collimator and the treatment couch can perform rotational motion allowing complex treatment delivery. For these rotations, the diameter of the smallest sphere containing all central beam axes is a measure for the effective movement of the isocenter, relative to the patient, throughout a treatment using different beam angles (Lutz *et al* 1988). The sphere is a consequence of apparatus misalignments, elastic deflections in the gantry structure and mechanical tolerances in the bearings. The effective movement of the isocenter has a similar effect on dose spread as spatially widening of the penumbra.

The isocenter travel can be measured in many different ways. Lutz *et al* (1988) proposed a method using a steel ball precisely located in the isocenter and rigid x-ray conical collimators for stereotactic radiosurgery. They captured the irradiation field and the radio-opaque steel ball projection on a film, on which the deviation between the field axis and the isocenter could easily be quantified for different rotation positions of the treatment unit. Already the combination between mechanical stability of the gantry and the alignment of the collimation device were merged in this test, which makes sense because the actual patient treatment mechanical accuracy is also a combination of these factors. Some variations exist of this

methodology (Low *et al* 1995, Tsai *et al* 1996, Karger *et al* 2001), some using the visual linac light field (Brezovich *et al* 1997) or the electronic portal imaging device instead of film (Dong *et al* 1997, Winkler *et al* 2003). Mamalui-Hunter *et al* (2008) and Mao *et al* (2011) extended the methodology to multiple markers in a calibration phantom to quantify the mechanical performance of a radiation therapy treatment unit. In the current image-guided radiation therapy era, some of these methods include measurement of the coincidence between integrated kV and MV imaging and the treatment beam. The work presented in this paper only focuses on the mechanical stability of the MV therapeutic beam.

One approach, used in many reports on rotational stability of the radiotherapy treatment beam, is the acquisition of a star shot film (Treuer *et al* 2000, Gonzalez *et al* 2004). Usually a radiosensitive film is placed in the plane of rotation and a sequence of narrow fields at different angles is exposing the film. The intersection of these fields forms a star-shaped pattern. Qualitatively, a lack of multi-axial symmetry of this pattern can already be an indication of mechanical instability of the rotation. The film also contains, be it more implicitly, high-resolution information about the radiation isocenter. Some publications on this subject (Treuer *et al* 2000, Gonzalez *et al* 2004) propose to apply computer-aided analysis of the star shot films. First, an automatic detection/segmentation of all the central axes of the individual star shot fields is performed. Even when the locus shape of isocenter travel may differ from a circle, a commonly used simplification is to assume a circular shape and perform a search for the smallest circle intersecting with all beam axes. The center of this circle is then called the radiation isocenter. The circle radius is called the radiation isocenter size, a quality measure for the rotational mechanical stability. When the instability contributions originate mainly from mechanical distortion and errors in beam axis segmentation, the intersection pattern will show an irregular shape. In the case of an appreciable systematic radial shift, resulting from an offset in the collimator to beam or beam to isocenter alignment, a more regular polygonal will be formed by the intersecting field axes.

The accuracy of the star shot approach depends on the field axis segmentation, mainly influenced by the noise in the film digitization, and the smallest circle detection algorithm. In most reports the latter was solved as a gradient-based optimization problem (Winkler *et al* 2003, Gonzalez *et al* 2004, Rosca *et al* 2006, Skworcow *et al* 2007). Treuer *et al* (2000) have mentioned a possible analytical solution to the smallest intersecting circle problem. This avoids the potential introduction of additional noise and uncertainties from the optimization approximation. They use the fact that the smallest circle intersecting a finite line set L of lines in the plane always occurs as the inscribing circle of three lines of L. Unfortunately the authors did not prove this property, that moreover only holds under certain conditions, neither did they settle the conditions that guarantee the existence and uniqueness of such a smallest circle. The intention of this paper is to provide the mathematical proofs that are missing in Treuer *et al* (2000) and present an algorithm which makes use of the analytical solution to the smallest intersecting circle problem for computer-aided star shot analysis. Additionally, the accuracy of an implementation of the algorithm was determined and the methodology was applied on star shots acquired on a wide range of treatment units with different designs. The mechanical stability was investigated in terms of radiation isocenter for O-ring-based gantry systems and some traditional cantilever or C-arm gantry designs. This work reports on mechanical performance of five different installations of the novel Vero system (Vero, BrainLab AG, Feldkirchen, Germany and Mitsubishi Heavy Industries, Ltd, Tokyo, Japan), an O-ring gantry system only recently introduced in the field, dedicated for stereotactic body radiation therapy (Kamino *et al* 2006, Depuydt *et al* 2011). To our knowledge this is the first report comparing different installations of this system in terms of the mechanical stability of the MV treatment beam.

2. Methods and materials

2.1. Acquisition of the star shot films

A star shot film is acquired by placing a radiation sensitive film in the rotation plane of the motion under investigation. The film is exposed to radiation from different angles of rotation such that the beams cross each other centrally in the film. The beams are typically collimated to a small field size in the film plane. The crossing of the different fields forms a star-shaped pattern on the film. As mentioned earlier, one way of interpreting a star shot film is to assess visually the multi-axial symmetry of this star pattern. This symmetry is directly related to mechanical stability of rotation when the star shot fields are evenly spread over the range of rotation angles. The computer-aided analysis of star shot films as described here does not use the central crossing pattern, but uses the central beam axis of the individual fields and recreates the crossing of the beam axes mathematically.

For gantry rotation, where the full 360° range is available for all treatment devices, in total five evenly spread beam angles of 216°, 288°, 0°, 72° and 144° were used, ordered clockwise. The field width was set to 1 cm, shaped by the MLC. For treatment couch rotation, the gantry was set fixed to 90° and the couch was rotating covering the angle range allowed by this gantry position. For the Vero system, where couch rotation is replaced by a rotation of the entire O-ring gantry around the vertical axis, the gantry angle was set fixed to 90° and the so-called ring rotation star shot was acquired instead. This Vero system and the Tomotherapy system (Tomotherapy/Accuray, Madison, WI, USA) do not allow rotation of the collimator separately. On the other C-arm gantry devices also the collimator rotation was measured with a star shot. Here, only the two central leaf pairs of the MLC were fully opened, forming a slit-shaped field. With again a set of evenly spread collimator angles, a star shot could be realized. On the Tomotherapy system only gantry rotation was measured using the static field option of the TomoDirect functionality (Reynders *et al* 2009). The wobble was measured using a similar approach as the collimator star shot; however, the slit-shaped field was given at 350° and 50° collimator rotation at gantry 0°, and the same at gantry 180°, forming a star shot of four slit fields.

2.2. Computer-aided analysis of the star shot films

The EBT2 radiochromic film (International Specialty Products, Wayne, NJ, USA) or, following chemical development, EDR2 radiographic film (Eastman Kodak Company, Rochester, NY, USA) were digitized using a commercial flatbed scanner, Epson 10000 XL, applying a 300 dpi pixel size (figure 1). A 16-bit grayscale scanning was used for the radiographic film. For a radiochromic film, a 48-bit color scan was acquired and only the red channel, having the highest overall response, was used for further processing. The beam axis positions were determined by acquiring cross sections of the field image in the film, and calculate the middle of the two full-width-half-maximum points on the cross section. This was repeated ten times per beam, five times at each side of the central star pattern crossing. Subsequently a linear model was fitted through these ten beam axis points, as can be seen in figure 2. To minimize the impact of noise in the film on the results, this process was repeated ten times per beam randomly varying cross-sectional positions. The median value of the linear model coefficients was taken as the final result for each beam axis location.

At this point, the star shot film information was reduced to a set of intersecting beam axes represented by the coefficients of linear equations. The quality metric used here is the radius of the smallest circle intersecting with all these lines. Different to most other reports which use gradient-based optimization for smallest circle searching, an analytical approach was applied

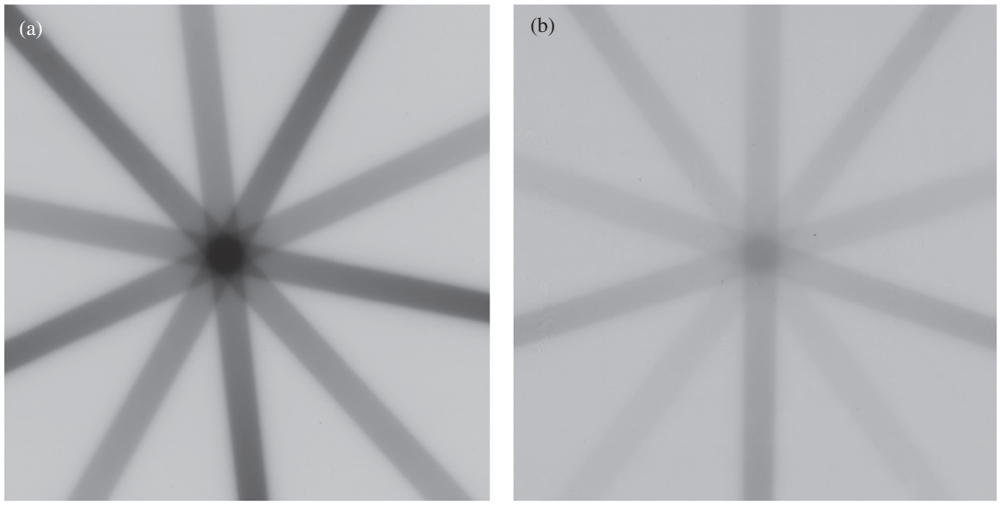

Figure 1. A star shot film acquired with (a) the Kodak EDR2 radiographic film, after development and digitization or (b) the ISP EBT2 radiochromic film. Both are exposed to 200 MU per beam.

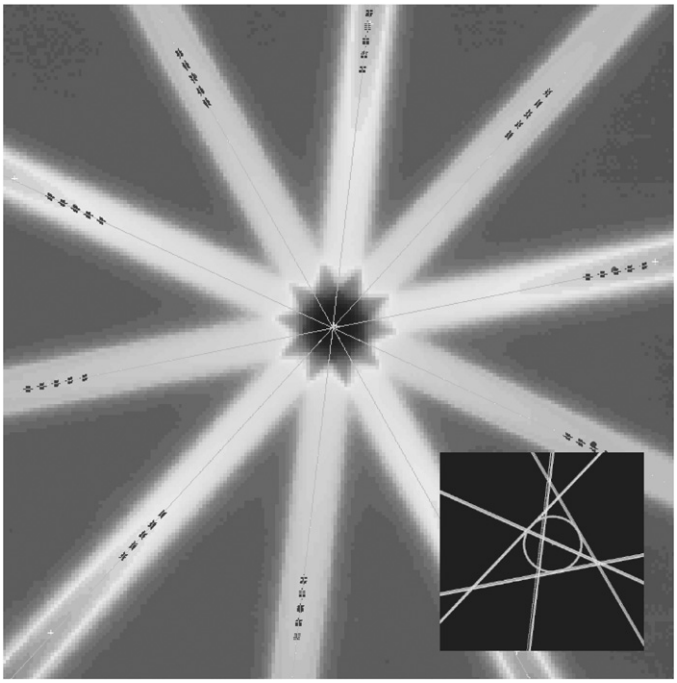

Figure 2. Star shot analysis, showing field axis segmentation. The inset shows the enlarged crossing of all detected beam axes and the calculated smallest intersecting circle, of which the radius is called the radiation isocenter size.

here. It can be proven mathematically (appendix) that the smallest intersecting circle always occurs as an inscribing circle of one of the possible triplet line subsets which can be made

from the complete set of beam axis lines. As such, the search algorithm constructs all these inscribing circles and selects the smallest one intersecting all beam axes.

2.3. Precision and accuracy of the algorithm

The rotational mechanical stability of state-of-the-art radiation therapy delivery equipment is typically below 0.5 mm. The accuracy and precision of the algorithm were investigated to confirm its adequacy to be used in these circumstances. Only with specialized equipment, to which the authors had no access, it would have been possible to create a gold standard reference mechanically. Here a similar approach was used as adopted by Gonzalez *et al* (2004) to create artificial star shots *in silico* for verification of the algorithm. Using a digitization of a developed blank film and superposition of artificially created beams, artificial star shot films were created. The advantage of this approach is that any given isocenter size can be introduced into the data. Noise characteristics were made similar to the levels seen in digitization of real film. The signal-to-noise ratios (SNRs) were varied in a wide range including those observed in actually acquired star shots with film and radiation. Divergence and attenuation of the beam were not included in the artificial star shot generation. The created artificial star shot data were fed to the algorithm and the results were compared to the *a priori* known radiation isocenter size, which was considered here as a gold standard reference.

Second, to investigate the influence of the scanning procedure and the film quality, five gantry angle star shots were acquired on the UZB Vero system, each with a stack of two identical films pressed together. Each film was digitized on the flatbed scanner multiple times and also under different orientations varying the angle with respect to the main axes of the scanner, and flipping sides of the film. The results of the analysis of the different films and different film orientations were compared to assess the reproducibility of the radiation isocenter size results. The above was performed for both the radiochromic and radiographic film types.

From the film stack measurements, the differences between the two films of every stack were calculated. Normal distribution for single film measurements was assumed because normality cannot be tested reliably on two sample data sets. For the difference distribution normality was verified using the Lilliefors test. From the distribution of the two film stack radiation isocenter size differences, first the standard deviation σ_{A-B} was calculated by multiplying the mean absolute difference by $\sqrt{}(\pi/2)$. Second, the standard deviation of the single film measurement distribution σ_A could be retrieved by dividing this by a factor $\sqrt{2}$, following from $\sigma_{A-B}^2 = \sigma_A^2 + \sigma_B^2$ and $\sigma_B = \sigma_A$. All the individually determined uncertainties were combined into one estimated total uncertainty of the method for both types of film separately.

To determine the relation between SNR of the beam images in film and the radiation exposure, expressed in monitor units (MU), some additional star shot measurements were performed varying the exposure in multiple steps from 12.5 to 300 MU per beam.

2.4. Application of the methodology in QC of different radiation therapy devices

A range of radiation therapy devices were subjected to the experiments described in the previous sections. In total five Vero systems, one Tomotherapy system and additionally four C-arm systems of different vendors and types were included in this study. On the Vero systems, the gantry and O-ring rotations and the gantry wobble were measured. On the Tomotherapy system only the gantry rotation could be tested. On the C-arm gantries, the gantry, collimator and couch rotations and the C-arm wobble were investigated. Both radiochromic and radiographic

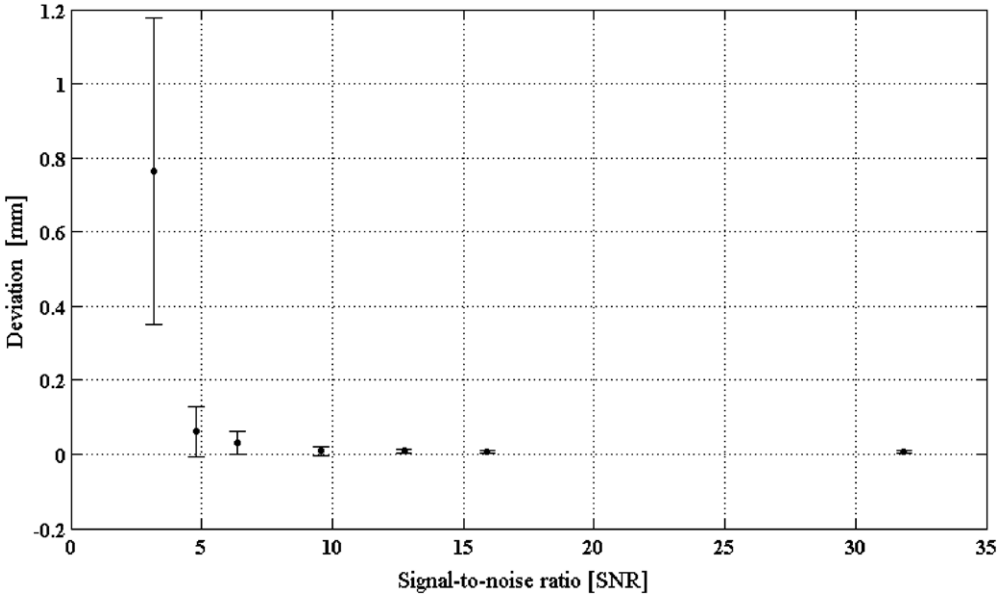

Figure 3. The deviation between the measured radiation isocenter size on the artificial star shots and the *a priori* known isocenter size, in function of the film SNR. The whiskers show the standard deviations on the measurements.

films were used for these experiments, depending on the film available in each participating hospital.

3. Results

3.1. Precision and accuracy of the algorithm

The noise level in both the radiochromic and radiographic films was measured after digitization. For a 200 MU exposure per angle, SNRs were observed of at least 20 for the radiochromic film, and at least 75 for the radiographic films. As the SNR is a good measure for the digitized film quality, this parameter was varied in the artificial star shots to quantify its impact on the accuracy of the algorithm. For each SNR level, five artificial star shots were generated in total, each with a different radiation isocenter size, all below 1.5 mm. In figure 3 the averages of the absolute errors between the known and the calculated isocenter sizes are plotted against the SNR. For SNRs above 10, the accuracy was fairly insensitive to changes in SNR, and the average errors remained below 0.007 mm (σ_1). Below an SNR of 10 the error increased rapidly. The measurements varying the film exposure showed that 87 and 32 MU were required for radiochromic and radiographic, respectively, to ensure a SNR of at least 10.

The influence in the digitization procedure of one single film by repeated scanning of the film, expressed in a standard deviation of the calculated isocenter size, was below 0.001 mm for the radiographic film and 0.005 mm for the radiochromic film. This increased to 0.006 and 0.02 mm (σ_2) when the orientation of the film was changed for each scan. Repeated analysis of the same digitization file introduced a spread of 0.001 and 0.005 mm, respectively (σ_3). The calculated single film uncertainty retrieved from the multiple film stack measurements was 0.02 mm for both film types (σ_4). A combination of the recorded uncertainties σ_i resulted

in an estimated overall uncertainty of 0.02 mm (σ) for radiographic film and 0.03 mm (σ) for radiochromic film.

3.2. Application of the methodology in QC of different radiation therapy devices

For the ten treatment units included in this study star shot films were acquired. All the data are compiled in table 1. Three of the five Vero systems, which were installed in 2010, showed similar behavior in terms of ring and gantry rotation. The two remaining Vero systems, installed in 2011, showed a reduction in isocenter size for gantry rotation, 0.12 and 0.25 mm compared to an average of 0.41 mm for the other three Vero systems. No major differences were seen for the ring rotation isocenter size. An appreciable C-arm wobble was observed in all C-arm systems. The C-arm wobble isocenter sizes ranged from 0.18 mm on the Truebeam system to 0.51 mm for the Elekta Infinity system (Elekta, Stockholm, Sweden), compared to 0.06 mm for the Vero O-ring. In terms of gantry rotation stability, the Varian Truebeam system (Varian Medical Systems, Palo Alto, CA, USA) showed the best performance with 0.09 mm isocenter size. The worst for this rotation was the Tomotherapy system with 0.87 mm. Collimator rotation isocenter radius was small for all systems. Couch rotation, on the C-arm systems, was only of considerable size for the Novalis system (BrainLab AG, Feldkirchen, Germany), 0.38 mm, and the Elekta Infinity system, 0.54 mm. For the latter, this somewhat reduced mechanical accuracy can probably be attributed to a known construction error of the concrete supporting the couch base plate. The error was corrected to meet the specifications before further installation of the accelerator system, however, possibly with a reduced level of quality.

4. Discussion

A methodology for computer-aided analysis of star shot films was refined and supported by a mathematical proof for the analytical solution of the smallest intersecting circle problem. An algorithm deploying this method was developed and subjected to accuracy/precision tests for two different types of commonly used radiosensitive film. Additionally, two groups of linac gantry designs were compared in terms of mechanical stability of gantry, collimator and couch rotation. The computer-aided analysis of star shot film consists of two steps. The first is finding the beam axes in the digitized film. The presented algorithm uses repeated analysis at random locations to reduce the effect of noise on beam axes detection. The second step, determining a smallest circle intersecting with all star shot beam axes, is classically handled as an optimization problem iteratively reducing the circle size. This possibly introduces additional noise into the results due to the limited resolution of the optimizer. In this work, the mathematical proof is provided for an analytical solution to the smallest intersecting circle problem, which does not introduce noise and as such increases accuracy of the star shot analysis.

The accuracy was tested for two types of film commonly available in a radiation therapy environment, the radiographic Kodak EDR2 film and the radiochromic ISP EBT2 film. The latter does not require chemical development and the result is readily available; however, spatial resolution and noise characteristics are affected by non-uniformities in the film (Hartmann *et al* 2010). Nevertheless, the analysis conducted in this work showed comparable performance for both types of film: an uncertainty of 0.04 mm (2σ) for the radiographic film and 0.06 mm (2σ) for the radiochromic film. This result indicates that the presented method is fairly independent of the quality of the film that is used for the measurement. Also, a considerable improvement was shown in terms of accuracy compared to Gonzalez *et al* (2004) reporting 0.2 mm (2σ) for

Table 1. The results of all radiation isocenter size measurements performed on different machine types in different institutions (BrainLab headquarters, UZ Brussel, Ospedale Sant'Anna Como, University of Texas Southwestern, European Institute of Oncology, UniversitätsSpital Zürich). Depending on the type of machine, only certain rotations could be measured.

Vendor	BrainLab/MHI					BrainLab/Varian	Varian	Elekta	Elekta	Tomotheraphy
Machine type	Vero	Vero	Vero	Vero	Vero	Novalis	Truebeam	Compac	Infinity	Hi Art
Gantry type	O-ring	O-ring	O-ring	O-ring	O-ring	C-arm	C-arm	C-arm	C-arm	O-ring
Site	BrainLab	UZB	Como	UTSW	IEO	UZB	USZ	UZB	UZB	UZB
Film type	EDR2	EDR2	EBT2	EBT2	EBT2	EDR2	EBT2	EDR2	EDR2	EDR2
Isocenter radius (mm)										
Gantry	0.39	0.40	0.43	0.12	0.25	0.28	0.09	0.23	0.26	0.87
Collimator	NA	NA	NA	NA	NA	0.03	0.09	0.01	0.01	NA
Ring	0.05	0.01	0.06	0.02	0.08	NA	NA	NA	NA	NA
Couch	/	/	/	/	/	0.38	0.03	0.09	0.54[a]	NA
Wobble	/	0.06	/	/	/	0.44	0.18	0.25	0.51	NA

[a] Base plate construction issue.

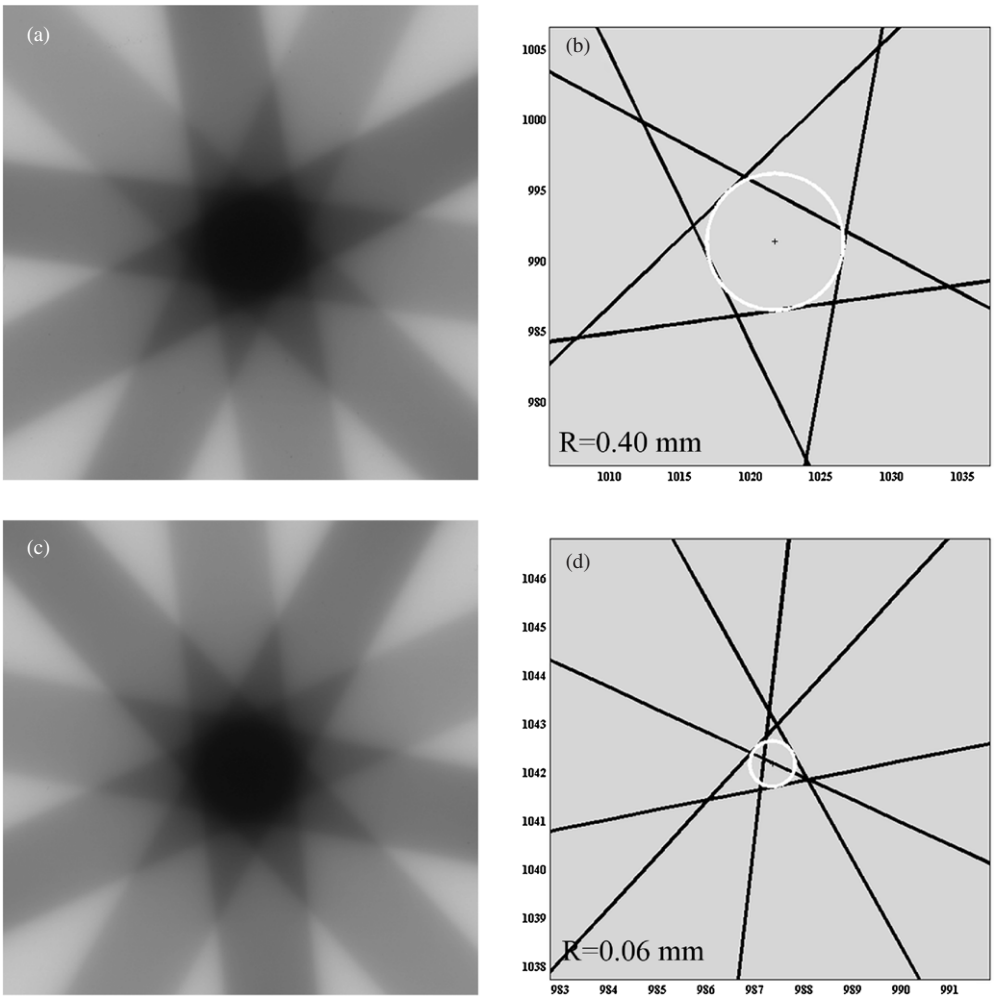

Figure 4. (a) The star shot patterns of the original acquisition on the UZB Vero system with (b) its analysis resulting in a radiation isocenter size calculation of 0.40 mm. (c) The acquisition after correction with an MLC shift of 0.4 mm resulted in an improvement to (d) 0.06 mm isocenter size.

a computer-aided star shot analysis. Measurement of radiation isocenter sizes below 0.2 mm now becomes possible with the improvements described in this work.

The main scope of this work was primarily to investigate the computer-aided star shot analysis using the analytical solution of the smallest circle problem. Additionally the method was applied in a study concerning mechanical rotation stability of a range of different radiotherapy treatment unit gantries. The fields used to acquire the star shots were collimated using the MLC. As such the results include misalignments of the MLC with respect to the beam. An example of this is shown in figure 4, where a star shot analysis is observed for the UZB Vero system. In figures 4(a) and (b) the initial analysis is shown resulting in an isocenter radius of 0.40 mm. It can be seen in figure 4(b) that the field axis lines form a regular polygon, which indicates a systematic misalignment of the field. After applying a shift of the MLC leafs by 0.4 mm, a second star shot was acquired resulting in more irregular beam

axes crossing or the so-called random walk and an isocenter radius reduction to 0.06 mm (figure 4(d)). This difference can also readily be observed in the improvement of multi-axial symmetry of the star pattern in figure 4(c) compared to figure 4(a), showing the sensitivity of the star shot method even using visual inspection only. The same correction experiment could be repeated on the Vero system sited at the BrainLab headquarters, suggesting a misalignment of the MLC with respect to the isocentric rotation embedded in the system calibration. For the more recent installations of the Vero system, this systematic misalignment was reduced. It is unclear whether the beam/MLC alignment procedure was modified or whether it can be attributed to the installation team gaining experience with this novel device. For the Vero system its gimbaled linac system (Kamino *et al* 2006, Depuydt *et al* 2011) is actively used to establish a better definition of the radiation isocenter through compensation of mechanical distortions during gantry rotation. The 0.06 mm radiation isocenter radius thus reflects most probably better Vero's intrinsic mechanical performance than the initial 0.40 mm. However, for actual patient treatments the system is only as accurate as the quality of the mechanical calibration of the MLC collimated treatment beam.

For tomotherapy a quantification of the tongue-and-groove/penumbral blurring effect is used to align MLC and linac (Balog *et al* 2003), with a reported accuracy of 0.7 mm. Balog *et al* also describe a 0°–180° gantry angle test to verify the alignment of the collimated beam with respect to the center of rotation for which a 1.5 mm tolerance level was proposed. Fenwick *et al* (2004) advised inclusion of a star shot film test in the three-monthly QC with a tolerance level of 1 mm. For helical tomotherapy dose delivery striving toward more stringent tolerance levels might not have a significant impact on the final dose delivery quality. However, for the novel static gantry beam delivery approach on the Tomotherapy device called TomoDirect (Reynders *et al* 2009), smaller tolerance levels for isocentric alignment might be appropriate.

Based on the data provided here, one could conclude that a limited accuracy of the calibration/alignment procedure influences the performance of the linac despite their high intrinsic mechanical accuracy. For this reason, a general conclusion of the comparison between mechanical stability of O-ring and C-arm designs remains inconclusive. When comparing the Vero isocenter size measurement with the best performing C-arm system, the Varian Truebeam, and accounting for the obtained accuracy of the measurement technique used in this study, the difference is too small to conclude to a significant difference in mechanical performance of both gantry designs.

The methodology described in this work can be used to monitor mechanical performance constancy of high-accuracy radiation treatment units. Besides determination of the isocenter size, the star shot film can be used as an accurate measurement of rotation angles. In general, film measurements in combination with computer-aided analysis can be used for a range of mechanical quality control of gantry, MLC but also couch translations and robotics couch rotations. An advantage over many other high-accuracy methods presented in other publications is that film and film digitizers or flatbed scanners are available in nearly all radiation therapy institutions. In combination with some fairly simple software, a highly accurate measurement tool becomes available for mechanical QC in clinical radiation therapy environments.

5. Conclusion

An analytical solution for the smallest intersecting circle problem was mathematically proven and applied in a computer-aided star shot film analysis tool. This resulted in a measurement procedure to assess mechanical rotational performance of high-accuracy radiotherapy treatment units. The technique was validated and used to compare mechanical

quality data of five different installations of the novel Vero system, a Tomotherapy system and a range of C-arm linacs. A potential advantage of O-ring gantries over C-arm gantries, in terms of mechanical stability of the treatment beam during rotation of the gantry, could not be confirmed. The application of computer-aided film analysis methodology can be further extended to other mechanics quality tests of radiation therapy linacs. The methodology described in this work can be used to monitor mechanical performance constancy of high-accuracy treatment devices, with means available in a clinical radiation therapy environment.

Acknowledgments

This collaborative work was supported by the Flemish government through the Hercules foundation and the 'Fonds voor Wetenschappelijk Onderzoek—Vlaanderen' grants G.0486.06 and G.0412.08, and corporate funding from BrainLab AG. The authors would like to thank Professor T R Mackie for valuable comments regarding the alignment of the Tomotherapy Hi Art unit. The authors also wish to thank Greg Aloupis, Sebastian Collette and Perouz Taslakian for their design of a linear algorithm for constructing the smallest intersecting circle. The idea of this algorithm significantly contributed to the composition of the proofs of the theorems in the appendix.

Appendix

In this appendix we prove the existence and uniqueness of the smallest intersecting circle for a regular line configuration in the plane. A planar configuration L of lines is called regular if it contains a finite number of lines, not all going through the same point, such that no two are parallel.

Furthermore, we will show that for a regular line configuration this circle is always tangent to three lines of L (figure 2).

Let us identify our workplane with the XY-plane in 3D space, given by the equation $z = 0$. Furthermore, we represent a circle C in this plane with center (x_0, y_0) and radius R as a point $p(C) = (x_0, y_0, R)$ in 3D space. Of course, such a point $p(C)$ always lies in the upper half-space $\mathrm{U} : \mathrm{z} \geqslant 0$, where the case $p(C)\ \square XY$ corresponds to a limit circle C with radius 0.

Next, with any line l in XY we can associate the two planes $\alpha_1(l)$ and $\alpha_2(l)$ that make an angle of 45° with XY. The half-spaces above these planes and bounded by these planes are denoted by $H_1(l)$ and $H_2(l)$, respectively. Note that the wedge $W(\mathrm{l}) = H_1(\mathrm{l}) \cap H_2(\mathrm{l})$ is completely contained in the upper half-space U. The following result is immediate:

Lemma A.1. *A circle C intersects a line l in XY if and only if the point p(C) lies in the wedge W(l).*

Suppose now we are given a finite configuration of lines in the plane, $L = \{l_1, \ldots, l_\mathrm{n}\}$. The hit region $W(L)$ of L is a polyhedral subset of U defined as $W(L) = W(l_1) \cap W(l_2) \cap \ldots \cap W(l_\mathrm{n})$ and it consists of exactly these points $p(C)$ that correspond to circles C intersecting every line of L. Clearly, such circles always exist and this proves that $W(L)$ is not empty for finite configurations. As a matter of fact, $W(L)$ is unbounded because there is no restriction on the radius of hitting circles.

The polyhedron $W(L)$ only meets XY if there exists a limit circle with zero radius that intersects every line in the configuration. Equivalently, this exactly occurs if there is a point that belongs to every member of L. We call L a star configuration if all its lines go through one point. Now we can state our existence theorem.

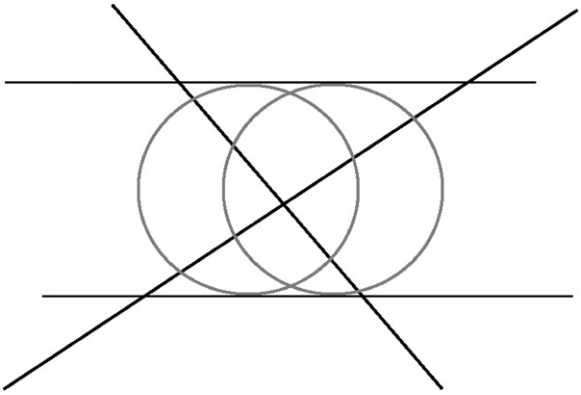

Figure A.1. Two possibilities are shown among the smallest intersecting circles for the given set of four lines.

Theorem A.2. *If a finite line configuration L is not a star, then there always exists a smallest hitting circle with nonzero radius.*

Proof. By lemma 1 we know that a circle C intersects all the lines of L if and only if $p(C)$ belongs to $W(L)$. Hence, smallest circles correspond to points in this polyhedron that have minimal z-coordinate. Because the region $W(L)$ is bounded in the vertical down direction (pointed by (0, 0, −1), z is minimized in $W(L)$, proving the existence of a smallest hitting circle. Furthermore, as L is not a star configuration, $W(L)$ lies strictly above XY. So, min(z) is achieved for a strictly positive z.

Although there always exists a smallest circle that intersects a given finite set of lines, it might be not the only one. This is illustrated in figure A.1. From the point of view of $W(L)$, multiple optimal solutions in this closed polyhedron for the objective direction given by (0, 0, −1) do arise if a face or edge of $W(L)$ is perpendicular to this direction or, equivalently, parallel to XY. From figure A.1 we learn that this might happen in case two (or more) lines of L are parallel. As a matter of fact, this appears to be the only case where the smallest hitting circle is not unique.

Recall that a regular configuration is a finite line configuration that is not a star and that does not contain parallel lines. □

Theorem A.3. *Each regular line configuration L has a unique smallest hitting circle with nonzero radius. Furthermore, this circle is tangent to at least three non-concurrent lines of L.*

Proof. Theorem 2 says that a regular line configuration always has a smallest hitting circle with nonzero radius. In order to prove that this circle is unique, it suffices to show that the polyhedron $W(L)$ contains no horizontal edges.

Observe that each edge of $W(L)$ lies on the line of intersection of two skew planes $\alpha_{\,i}(l_1)$ and $\alpha_{\,j}(l_2)$ associated with lines l_1 and l_2 in L ($1 \leqslant i, j \leqslant 2$). Also note that $l_1 \neq l_2$,because $\alpha_{\,1}(l) \cap \alpha_{\,2}(l) = l$, but l lies in XY, while $W(L) \cap XY =$ empty for regular configurations.

A possible horizontal edge of $W(L)$ would lie on a horizontal line k in some plane $\alpha_i(l)$. But such a line k is the intersection of $\alpha_i(l)$ with a horizontal plane. So, k and l are obtained by intersecting the same plane by two parallel planes, whence $k \,//\, l$. Consequently, if $\alpha_i(l_1)$ and $\alpha_j(l_2)$ intersect in a horizontal line k, then k is parallel to both l_1 and l_2. But this yields $l_1 \,//\, l_2$, which is excluded for regular line configurations.

We conclude that there is exactly one point $P = p(C)$ in the region $W(L)$ with minimal z-coordinate and that this point must be a vertex of $W(L)$. Such a vertex P always occurs as intersection of at least three planes $\alpha_i(l)$ associated with three lines in L. Note also that these three lines are non-concurrent, because otherwise the intersection P of the associated planes lies in XY and that is impossible. This proves that the corresponding optimal circle C is tangent to three non-concurrent lines. □

Remark. More details on the geometric properties and algorithms for the minimal intersecting circle of a line configuration can be found in Penne *et al* 2011 Here we provide, among other things:

- The proof that the minimal intersecting circle of a regular configuration always occurs as inscribed circle of a triangle formed by three of its lines.
- The proof that an inscribed circle to three lines of a regular configuration, moreover intersecting the whole configuration, must be the unique smallest intersecting circle.
- The proof that the minimal intersecting circle of a regular configuration always occurs as the largest of all inscribed circles to one of its triangles.
- An O(n) time algorithm to compute a smallest intersecting circle for a finite line configuration.

References

Balog J *et al* 2003 Benchmarking beam alignment for a clinical helical tomotherapy device *Med. Phys.* **30** 1118–27

Brezovich I *et al* 1997 Quality assurance system to correct for errors arising from couch rotation in linac-based stereotactic radiosurgery *Int. J. Radiother. Oncol. Biol. Phys.* **38** 883–90

Depuydt T *et al* 2011 Geometric accuracy of a novel gimbals based radiation therapy tumor tracking system *Radiother. Oncol.* **98** 365–72

Dong L *et al* 1997 Verification of radiosurgery target point alignment with an electronic portal imaging device (EPID) *Med. Phys.* **24** 263–7

Fenwick J *et al* 2004 Quality assurance of a helical tomotherapy machine *Phys. Med. Biol.* **47** 2933–53

Gonzalez *et al* 2004 A procedure to determine the radiation isocenter size in a linear accelerator *Med. Phys.* **31** 1489–93

Hartmann B *et al* 2010 Homogeneity of Gafchromic® EBT2 film *Med. Phys.* **37** 1753–56

ICRU 2010 Prescribing, recording, and reporting photon-beam intensity-modulated radiation therapy (IMRT) *ICRU Report 83* (Oxford: Oxford University Press)

Kamino Y *et al* 2006 Development of a four-dimensional image-guided radiotherapy system with a gimbaled x-ray head *Int. J. Radiat. Oncol. Biol. Phys.* **66** 271–8

Karger C *et al* 2001 A method for determining the alignment accuracy of the treatment table axis at an isocentric irradiation facility *Phys. Med. Biol.* **46** N19–26

Low D *et al* 1995 Minimization of target positioning error in accelerator-based radiosurgery *Med. Phys.* **22** 443–8

Lutz W *et al* 1988 A system for stereotactic radiosurgery with a linear accelerator *Int. J. Radiother. Oncol. Biol. Phys.* **14** 373–81

Mamalui-Hunter M *et al* 2008 Linac mechanic QA using a cylindrical phantom *Phys. Med. Biol.* **53** 5139–49

Mao *et al* 2011 Initial application of a geometry QA tool for integrated MV and kV imaging systems on three image guided radiotherapy systems *Med. Phys.* **38** 2335–41

Penne R *et al* 2011 A study of the smallest circle intersecting a given line configuration *Technical Report* IWT 2011–02 ISSN 2032–0450

Reynders T *et al* 2009 Dosimetric assessment of static and helical tomotherapy in the clinical implementation of breast cancer treatments *Radiother. Oncol.* **93** 71–9

Rosca F *et al* 2006 An MLC-based linac QA procedure for the characterization of radiation isocenter and room lasers' position *Med. Phys.* **33** 1780–7

Skworcow P *et al* 2007 A new approach to quantify the mechanical and radiation isocentres of radiotherapy treatment machine gantries *Phys. Med. Biol.* **52** 7109–24

Treuer H *et al* 2000 On isocentre adjustment and quality control in linear accelerator based radiosurgery with circular collimators and room lasers *Phys. Med. Biol.* **45** 2331–42

Tsai J *et al* 1996 The measurement of linear accelerator isocenter motion using a three-micrometer device and an adjustable pointer *Int. J. Radiother. Oncol. Biol. Phys.* **34** 189–95

van Herk M *et al* 2004 Errors and margins in radiotherapy *Semin. Radiat. Oncol.* **14** 52–64

Winkler P *et al* 2003 Introducing a system for automated control of rotation axes, collimator and laser adjustment for a medical linear accelerator *Phys. Med. Biol.* **48** 1123–32